Phys. Status Solidi RRL **3**, No. 7–8, 230–232 (2009) / **DOI** 10.1002/pssr.200903221

pss +++rapid research letters+++
www.pss-rapid.com

Micro-photoluminescence spectroscopy on metal precipitates in silicon

Paul Gundel[*,1], Martin C. Schubert[1], Wolfram Kwapil[1], Jonas Schön[2], Manfred Reiche[3], Hele Savin[4], Marko Yli-Koski[4], Juan Angel Sans[5], Gema Martinez-Criado[5], Winfried Seifert[6], Wilhelm Warta[1], and Eicke R. Weber[1]

[1] Fraunhofer Institute for Solar Energy Systems (ISE), Heidenhofstr. 2, 79110 Freiburg, Germany
[2] Freiburg Materials Research Center, University of Freiburg, Stefan-Meier-Str. 21, 79104 Freiburg, Germany
[3] Max Planck Institute for Microstructure Physics, Weinberg 2, 06120 Halle, Germany
[4] Helsinki University of Technology, P.O. Box 3500, 02015 TKK, Finland
[5] ESRF, 6 rue Jules Horowitz, BP 220, 38043 Grenoble Cedex, France
[6] IHP/BTU Joint Lab, BTU Cottbus, Konrad-Wachsmann-Allee 1, 03046 Cottbus, Germany

Received 20 July 2009, revised 7 August 2009, accepted 10 August 2009
Published online 13 August 2009

PACS 61.72.Hh, 78.30.Am, 78.55.Ap, 78.70.En

[*] Corresponding author: e-mail paul.gundel@ise.fraunhofer.de

Metallic impurities are detrimental to many silicon devices and limit the efficiency of multicrystalline silicon solar cells. Therefore they are a major subject of ongoing research. Photoluminescence spectroscopy is a promising technique for detecting precipitated metals in silicon because of its sensitivity to the minority carrier density and to specific types of defects; however the impact of impurities on the defect luminescence could not be clarified yet. In this letter we examine the role of micron-sized iron and copper precipitates in direct bonded wafers by micro-photoluminescence spectroscopy. Both kinds of precipitates are detectable by means of the reduced band-to-band luminescence. An element-specific effect on the defect luminescence is observed. The results are confirmed by X-ray fluorescence spectroscopy.

1 Introduction The performance of many silicon devices heavily depends on the metal contamination. In particular the efficiency of solar cells made of block-cast multicrystalline (mc) silicon with its inevitable high transition metal content is significantly reduced. Two of the most common and at the same time detrimental impurities are iron and copper. While at least the interstitial iron concentration is detectable with minority carrier lifetime measurement techniques [1, 2], the detection of single metal precipitates is only possible with technically demanding methods such as X-Ray Fluorescence spectroscopy (XRF) [3] or Transmission Electron Microscopy (TEM), which requires a time-consuming sample preparation and pre-characterisation [4]. The precipitation of metals is relevant for mc silicon solar cells in many ways: Metal precipitation at crystal defects during the crystal growth can clean grains from impurities and thus, improve the performance [5], or can cause shunts and sites of pre-breakdown and damage the cell or module respectively [6, 7]. These effects make the development of an accessible, fast and non-destructive technique for the detection of metal precipitates highly relevant for the further improvement of mc silicon solar cells. A promising approach for the detection of metal precipitates is photoluminescence (PL) spectroscopy with a high spatial resolution. PL spectroscopy provides complementary material parameters in one measurement: The intensity of the band-to-band (BB) peak is a qualitative measure for the recombination activity [8], the intensity and energy position of the defect PL peaks between 0.8 eV and 0.99 eV at room temperature or below yield additional information about the nature of the defects [9, 10]. The role of impurities in the defect PL has been widely discussed [11], but is far from being clarified yet. To obtain meaningful experimental results our study is based on well defined samples and maximum spatial resolution. As highly defined samples we choose Direct Bonded Wafers (DBWs) [12], whose clean dislocation networks represent an ideal model system for mc silicon. The DBWs are con-

taminated with iron or copper, which precipitate at the dislocation network or close to the interface. These defect systems, which consist of the dislocation network and the metal precipitates, are examined with micro-PL spectroscopy at ambient temperature and the results are compared to XRF measurements with similar resolution, which were conducted at ID22 at the European Synchrotron Radiation Facility (ESRF).

2 Experimental Details on the preparation of the DBWs can be found in [12]. For this work two 600 µm thick n-type float-zone wafers with a phosphorous doping below 10^{13} cm^{-3} were taken as starting material for the bonding. The DBWs are contaminated either with iron or with copper by in-diffusion at 1030 °C and 1200 °C respectively. In addition, a reference DBW is subject to the same heat treatment without any contamination. For the analysis of cross contamination effects one DBW is contaminated with iron and copper with the same heat treatment as for the iron contamination.

After the in-diffusion the contaminants are allowed to precipitate at the dislocation network within 2 h at approximately 850 °C. Finally the DBWs are prepared with a bevelled polish and a subsequent surface cleaning etch in order to allow PL measurements at the dislocation network. The PL spectroscopy setup is a confocal microscope with an excitation laser (532 nm wavelength) with a power of 10 mW on the sample. The PL light is split up by a 150 g mm^{-1} grating and detected by an InGaAs detector. For these experiments a 50× lens with a resulting depth of focus of 3 µm is used. This confocal setup provides a radial resolution of about 0.8 µm and a spectral resolution of 0.5 nm. The XRF measurements were conducted with a 10 keV X-ray microbeam at the beamline ID22 of the ESRF. The hard X-ray microprobe provides a spatial resolution of 4 µm in the horizontal and 1 µm in the vertical direction.

3 Results In the iron contaminated sample the intensity of the BB PL peak is reduced at the dislocation network (which intersects the surface of the bevelled sample to the right side of the blue line in Fig. 1a) due to its recombination activity. At some distinct spots of a size between 1 µm and 4 µm the BB PL peak is particularly low (circles in Fig. 1a). At these spots iron precipitates were detected by XRF (Fig. 1b). Both measurements show a good agreement though the escape depth of the PL is smaller than the information depth of the fluorescence, which demonstrates the potential of micro-PL spectroscopy to detect precipitates due to their increased recombination activity. As expected, XRF did not detect any impurities other than iron in this sample. The dashed circle shows a limitation of the micro-PL setup. The sensitivity is limited to an area close to the surface because of the short absorption length of the excitation laser (about 1 µm). Since the iron precipitate in the dashed circle lays deeper in the sample, it cannot be detected by the current micro-

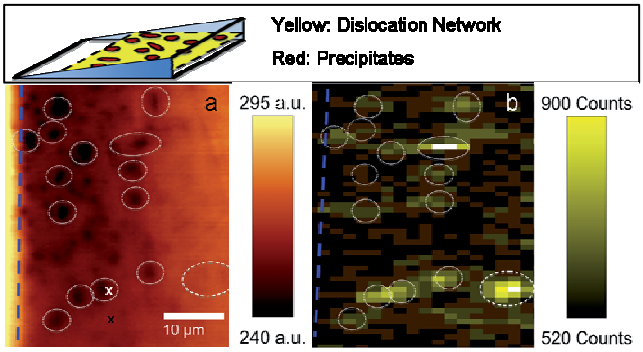

Figure 1 (online colour at: www.pss-rapid.com) Top: Scheme of the sample preparation with the polished angle. Bottom: Intensity of the BB PL peak at room temperature (a) and of the iron X-ray Kα fluorescence (b). The dislocation network intersects the surface to the right of the dashed blue line. The spots with reduced BB PL intensity (white circles) are caused by recombination active precipitates, which were detected with XRF (b). The PL measurement clearly shows more details than the XRF measurement, which suggests a higher sensitivity.

PL setup. This limitation might be overcome by an excitation laser with a longer wavelength and absorption length in silicon.

The iron precipitates alter not only the BB PL but also the defect PL. In Fig. 2 four normalised PL spectra are compared: (1) At an iron precipitate (white × in Fig. 1a), (2) at a position without precipitate (black × in Fig. 1a), (3) the reference DBW, which was subject to the same temperature steps as the iron contaminated sample, without contamination and (4) at a copper precipitate (white × in Fig. 4a).

The iron contaminated sample shows an enhanced defect PL at 1.3 µm compared to the uncontaminated sample,

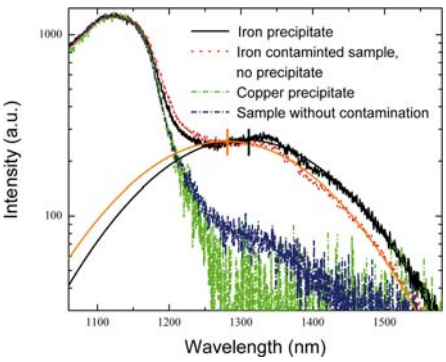

Figure 2 (online colour at: www.pss-rapid.com) Comparison of the normalised room temperature PL spectra at an iron precipitate (white × in Fig. 1a), at a position without precipitate (black × in Fig. 1a), the bonded wafer without contamination and at a copper precipitate (white × in Fig. 4a). The defect PL at the iron precipitate is shifted to longer wavelengths, which can be seen from the fit of the defect PL (thin orange curve – no precipitate, thin black curve – precipitate) with the thick vertical lines marking the peak positions. The BB peak is also fitted, but the fit function is not shown for the sake of clarity.

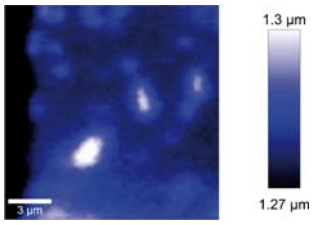

Figure 3 (online colour at: www.pss-rapid.com) This figure shows the position of the Gauss peak (compare to Fig. 2), which fits the defect PL. A clear shift to longer wavelengths at iron precipitates can be observed. Shown is a detail from the lower left side of Fig. 1a. This figure demonstrates the ability of PL spectroscopy to identify precipitates in the size of 1 µm or smaller, since the signal might be broadened.

when the spectra are normalized to the BB PL. The spectra are multiplied by the factors: 1 for the iron precipitate, 0.72 for the iron contaminated sample at no precipitate, 7.8 for the copper precipitate and 0.74 for the uncontaminated sample. In the copper contaminated sample the defect PL is drastically reduced.

At the iron precipitate the broad defect PL band is shifted to longer wavelengths. If this is due to an additional peak with a longer wavelength, which is suggested by the decreased quality of the fit for the defect PL with one Gauss peak (see Fig. 2), or due to an energy shift of the peak cannot be conclusively decided from these data. The defect PL is weaker in the uncontaminated sample.

In a sample with copper and iron contamination where both iron and copper were precipitated at the dislocations, the spectrum is a composition between the pure iron and pure copper spectrum. The effect of the defect PL shift at precipitates is demonstrated for a detail from the lower left side of Fig. 1 with longer integration times in Fig. 3. For this the entire spectrum was fitted at each point with four Gauss peaks (three for the BB peak and one for the defect PL). The shift to higher wavelengths at the iron precipitates can be clearly seen and is higher for comparatively big precipitates.

While the defect PL is almost completely suppressed in all of the sample with only copper, the intensity of the BB PL peak can be used to locate the copper precipitates at the dislocation network, which is demonstrated by the comparison to the intensity of the copper Kα X-ray fluorescence in Fig. 4. At 4.2 K the suppression of defect PL by high copper concentrations was reported in [13].

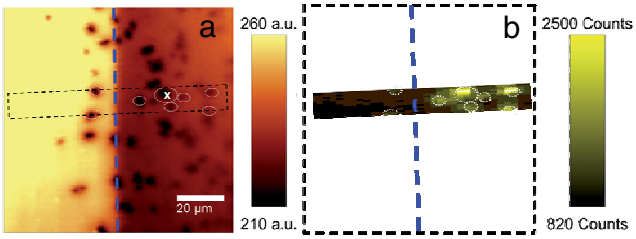

Figure 4 (online colour at: www.pss-rapid.com) Intensity of the PL BB peak on the left side (a) and the intensity of the copper Kα X-ray fluorescence (b). The dislocations are on the left to the blue dashed line. The spots with decreased PL BB peak intensity (white circles) can be clearly correlated to the copper precipitates, which are identified by XRF (b).

4 Conclusion In this paper we showed that micro-photoluminescence is an excellent tool for identifying metal precipitates in silicon. The minimum size for the detection is 1 µm or even smaller, since the PL signal might be broadened. By plotting the intensity of the BB PL peak the position of precipitates correlates to spots of decreased intensity. This was demonstrated for contaminated direct bonded wafers by comparison with XRF. Iron and copper were found to have a different effect on the defect PL around 1.3 µm at room temperature. While the defect PL was increased in the iron contaminated sample and shifted to longer wavelength at iron precipitates, it is suppressed in the copper contaminated sample. This dependence of the defect PL on the contaminant may be utilized in order to identify the chemical composition of precipitates. So far the detection of precipitates is limited to near surface precipitates. This limitation might be overcome by an excitation laser with a longer wavelength and a longer absorption length in silicon.

Acknowledgements We gratefully acknowledge M. Hecht, M. Kwiatkowska, H. Lautenschlager, R. Neubauer, and G. Räuber for sample preparation. We acknowledge the European Synchrotron Radiation Facility for provision of synchrotron radiation facilities at ID22. This work was funded by the project Silicon Beacon.

References

[1] G. Zoth and W. Bergholz, J. Appl. Phys. **67**, 6764 (1990).
[2] D. Macdonald, J. Tan, and T. Trupke, J. Appl. Phys. **103**, 073710 (2008).
[3] T. Buonassisi, M. Heuer, A. A. Istratov, M. D. Pickett, M. A. Marcus, and E. R. Weber, Acta Mater. **55**, 6119 (2007).
[4] S. Sadamitsu, A. Sasaki, M. Hourai, S. Sumita, and N. Fujino, Jpn. J. Appl. Phys. **30**, 1591 (1991).
[5] J. Bailey and E. R. Weber, Phys. Status Solidi A **137**, 515 (1993).
[6] V. Hoffmann, K. Petter, J. Djordjevic-Reiss et al., in Proc. of 23rd EU-PVSEC, Valencia, 2008 (unpublished).
[7] J. Isenberg and W. Warta, J. Appl. Phys. **95**, 5200 (2004).
[8] P. Würfel, J. Phys. C **15**, 3967 (1982).
[9] H. Sugimoto, K. Araki, M. Tajima, T. Eguchi, I. Yamaga, M. Dhamrin, K. Kamisako, and T. Saitoh, J. Appl. Phys. **102**, 054506 (2007).
[10] M. Suezawa and K. Sumino, Phys. Status Solidi A **78**, 639 (1983).
[11] M. Inoue, H. Sugimoto, M. Tajima, Y. Ohshita, and A. Ogura, J. Mater. Sci., Mater. Electron. **19**, S132 (2008).
[12] M. Kittler, X. Yu, O. F. Vyvenko, M. Birkholz, W. Seifert, M. Reiche, T. Wilhelm, T. Arguirov, A. Wolff, W. Fritzsche, and M. Seibt, Mater. Sci. Eng. C **26**, 5–7 (2006).
[13] E. C. Lightowlers and V. Higgs, Phys. Status Solidi A **138**, 665 (1993).

